

Momentum-resolved resonant inelastic X-ray scattering on a single crystal under high pressure

Masahiro Yoshida,^{a,b*} Kenji Ishii,^b Ignace Jarrige,^b Tetsu Watanuki,^b Kazutaka Kudo,^c Yoji Koike,^d Ken'ichi Kumagai,^e Nozomu Hiraoka,^f Hirofumi Ishii,^f Ku-Ding Tsuei^f and Jun'ichiro Mizuki^{b,g}

^aDepartment of Physics, Tohoku University, Sendai 980-8578, Japan, ^bSpring-8, Japan Atomic Energy Agency, Sayo, Hyogo 679-5148, Japan, ^cDepartment of Physics, Okayama University, Okayama 700-8530, Japan, ^dDepartment of Applied Physics, Tohoku University, Sendai 980-8579, Japan, ^eDepartment of Physics, Hokkaido University, Sapporo 060-0810, Japan, ^fNational Synchrotron Radiation Research Center, Hsinchu 30076, Taiwan, and ^gSchool of Science and Technology, Kwansai Gakuin University, Sanda, Hyogo 669-1337, Japan.

*E-mail: yoshimasa@kwansai.ac.jp

A single-crystal momentum-resolved resonant inelastic X-ray scattering (RIXS) experiment under high pressure using an originally designed diamond anvil cell (DAC) is reported. The diamond-in/diamond-out geometry was adopted with both the incident and scattered beams passing through a 1 mm-thick diamond. This enabled us to cover wide momentum space keeping the scattering angle condition near 90°. Elastic and inelastic scattering from the diamond was drastically reduced using a pinhole placed after the DAC. Measurement of the momentum-resolved RIXS spectra of Sr_{2.5}Ca_{11.5}Cu₂₄O₄₁ at the Cu *K*-edge was thus successful. Though the inelastic intensity becomes weaker by two orders than the ambient pressure, RIXS spectra both at the center and the edge of the Brillouin zone were obtained at 3 GPa and low-energy electronic excitations of the cuprate were found to change with pressure.

Keywords: resonant inelastic X-ray scattering; electronic excitations; high pressure; diamond anvil cell.

© 2014 International Union of Crystallography

1. Introduction

Resonant inelastic X-ray scattering (RIXS) stands out as a powerful element- and orbital-specific probe of the electronic excitations between the occupied and unoccupied valence-band states (Ament *et al.*, 2011), which has been rapidly developed by utilizing third-generation radiation X-rays. Since then, RIXS has achieved significant progress in condensed matter physics. It is sensitive to local (*e.g.* crystal-field) (Ishii *et al.*, 2011), nearest-neighboring (*e.g.* charge transfer) (Kao *et al.*, 1996; Hasan *et al.*, 2000; Kim *et al.*, 2010) and collective (*e.g.* magnons) interactions (Hill *et al.*, 2008), making it a comprehensive tool for the electron–electron interactions. When using a single-crystal sample, RIXS studies can be performed in a momentum-resolved manner. This is the most important advantage of RIXS when compared with other optical methods.

Another advantage of RIXS, particularly in the hard X-ray regime, is the large penetration length of photons. It not only ensures the bulk sensitivity of the observed spectra but also naturally leads us to extend the RIXS technique to measurement under extreme environments because the study of physical properties of materials under extreme environments

is of central importance in condensed matter physics. In particular, pressure is one of the most important external parameters as it is a clean and efficient way to directly alter the interatomic distance, hence the hybridization and the band width, which in turn affect drastically the physical properties. Therefore, experimental techniques for studying valence electronic states through the observation of low-energy excitations under high pressure are in high demand. Momentum resolution is further required for detailed studies of the electronic band structure of crystalline materials. In this respect RIXS perfectly matches the requirements, and a diamond anvil cell (DAC), which is commonly used as a device for generating high pressure, is suitable for this purpose.

Shukla *et al.* (2003) and Rueff & Shukla (2010) have performed pioneering high-pressure RIXS experiments using a DAC and observed excitations of valence electrons in NiO and CoO. However, they measured polycrystalline samples, so that the advantage of momentum resolution was not exploited completely. To the best of our knowledge, momentum-resolved RIXS studies under high pressure have not yet been reported on single crystals. On the other hand, several works of non-resonant inelastic X-ray scattering (NIXS) using DACs have been performed to measure phonons under high pres-

sure (Raymond *et al.*, 2002, 2011; Farber *et al.*, 2006; Loa *et al.*, 2007). A common experimental difficulty of NIXS and RIXS experiments using single crystals under high pressure is disentanglement of the signal arising from the sample and the parasitic signal from the high-pressure gasket or the diamond around the sample. The parasitic signal might be larger in RIXS because the photon energy of RIXS (~ 9 keV in the present study) is much lower than that of non-resonant IXS which is typically above 20 keV and hence reduces incident photon intensity on the sample. Furthermore, the lower photon energy imposes additional constraints on the experimental geometry. For example, transmission geometry is almost impossible in RIXS. When one keeps the scattering angle close to 90° to minimize the elastic scattering, the geometrical restriction is further severe.

Here we overcome these difficulties and report the first demonstration of the momentum-resolved RIXS to a single crystal under high pressure. To this end we have used a DAC specially designed to accommodate the RIXS geometry requirements while avoiding the parasitic signal from the gasket, by enabling to work in the reflection geometry with both incoming and scattered X-rays passing through the same diamond. Focus of the incoming beam was achieved using Be refractive lenses and a pinhole was placed to suppress scattering from the diamond. The sample is a single crystal of the two-leg ladder cuprate, $\text{Sr}_{14-x}\text{Ca}_x\text{Cu}_{24}\text{O}_{41}$, a composite system in which Cu_2O_3 two-leg ladders and CuO_2 chains coexist with a different periodicity and the two-leg ladder is responsible for the conductivity. This choice is motivated both by the relatively strong RIXS signal previously observed on this system at ambient pressure (~ 15 counts s^{-1} for the Mott gap excitation) (Ishii *et al.*, 2007), and by reports that its physical properties vary greatly with external and/or chemical pressure, that is, an insulator–metal transition takes place at about 6 GPa for $x = 0$ and superconductivity sets in at around 3 GPa for $x \geq 9$ (Kojima *et al.*, 2001). These two phenomena call for a study of the momentum dependence of the electronic structure of $\text{Sr}_{14-x}\text{Ca}_x\text{Cu}_{24}\text{O}_{41}$ as a function of pressure, which we show in this paper for $x = 11.5$.

2. Experimental set-up

2.1. Beamline optics

RIXS experiments were performed at BL11XU of SPring-8. Incident X-rays were monochromated by a double-crystal Si(111) monochromator and a secondary Si(400) channel-cut monochromator. The incident X-ray energy was tuned to 8993 eV where charge excitations are resonantly enhanced (Ishii *et al.*, 2007). Scattered X-rays were analyzed in energy by a spherically bent diced Ge(733) crystal on a Rowland circle of 2 m in diameter. The total energy resolution estimated from the full width at half-maximum (FWHM) of the elastic peak was about 500 meV. While a horizontal focus of $45 \mu\text{m}$ is achieved for the incoming beam with a cylindrical mirror, for this experiment we have added compound refractive lenses made of beryllium (Be lenses) after the Si(111) mono-

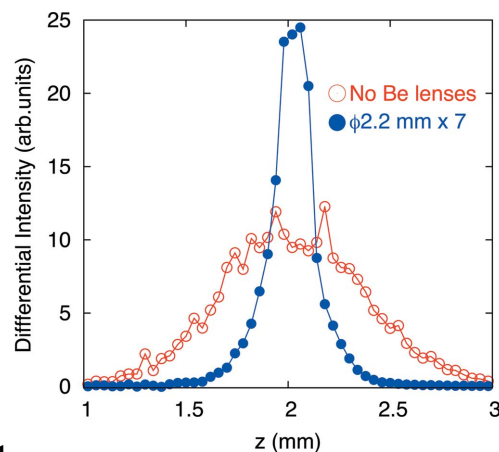


Figure 1 Beam size evaluated by the knife-edge method. The spectra with open and filled circles are measured without and with the Be lenses, respectively.

chromator in order to focus the beam vertically (Snigirev *et al.*, 1996; Protopopov & Valiev, 1998). The Be lenses consist of seven holes of diameter 2.2 mm drilled in a Be block. The focal length is about 18.9 m, very close to the distance between the lenses and the sample position, 19 m. The performance of the Be lenses was checked by measurement of the vertical focus at the sample position using the knife-edge method, shown in Fig. 1. The open and filled profiles show the result of the knife-edge scan without and with the Be lenses, respectively. The vertical FWHM is found to decrease by a factor of four, from 800 to 200 μm , when using the Be lenses, confirming their adequacy.

2.2. Sample environment

Scattering and spectroscopic high-pressure experiments are often performed in the in-plane geometry with both incoming and scattered X-rays going through a Be gasket, owing to the low X-ray absorption of Be and the wide optical access (Hemley *et al.*, 1997). However, Be being a metal, its loss spectrum shows several excitations between 0 and a few eV, and is therefore unsuitable for RIXS experiments. Because diamond is transparent up to about 6 eV loss, we decided to use a diamond-in/diamond-out geometry. The sample was loaded in the DAC as shown in Fig. 2, which has two custom-designed features to be fully compatible with the geometrical requirements of a single-crystal RIXS experiment. One is a large horizontal opening angle on one side of the cell to access wide momentum space keeping the condition of scattering angles near 90° . The condition minimizes the intensity of the elastic scattering, as the scattering plane is parallel to the polarization of the incident photons. The opening angles of the cell used in the present study are about 100° and 30° in the horizontal and vertical, respectively, and enabling us to cover the entire Brillouin zone of the ladder (*ac*) plane of $\text{Sr}_{14-x}\text{Ca}_x\text{Cu}_{24}\text{O}_{41}$. The other is asymmetric thickness of the diamonds, 1.0 and 1.5 mm. In this diamond-in/diamond-out geometry the absorption effect by the diamond cannot be ignored. To minimize the absorption of X-rays by the

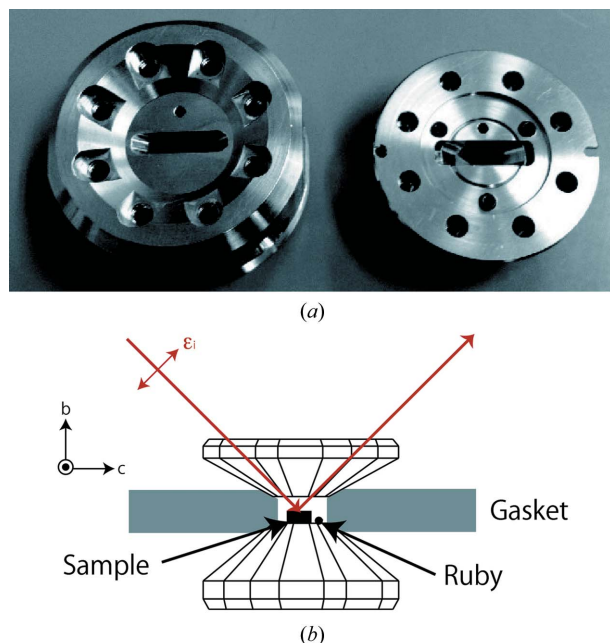


Figure 2
 (a) Photograph of the diamond anvil cell. (b) Schematic of the DAC. The solid line through the upper diamond shows the practical optical pass.

diamond, both the incident and scattered beams pass through the thinner diamond as shown in Fig. 2(b). The path length of X-rays in the diamond anvil is $2\sqrt{2}$ times as long as the thickness of the diamond under practical experimental conditions: the incident and outgoing angles are 45° and the scattering angle is 90° . In this configuration we gain a factor of four in intensity, which is estimated from the transmission ratio of the 1 mm diamond to the 1.5 mm diamond for the respective path length. Here we used the absorption coefficient of diamond (about 10.6 cm^{-1} at 8980 eV; Sasaki, 1990). Pressure was evaluated by the ruby-fluorescence method (Piermarini *et al.*, 1975). A 1:1 mixture of Fluorinert F70 and F77 was used as the pressure-transmitting medium. The culet diameter of the diamond was 1 mm. A gasket made of stainless steel SUS301 was used, with a sample chamber of diameter 500 μm .

Single crystals of $\text{Sr}_{14-x}\text{Ca}_x\text{Cu}_{24}\text{O}_{41}$ ($x = 0, 11.5$) were grown by the traveling-solvent floating-zone method. The polished surface of a piece $120 \mu\text{m} \times 300 \mu\text{m} \times 70 \mu\text{m}$ in size was placed on the culet of the 1.5 mm-thick diamond, mounted so that the bc plane is almost parallel to the scattering plane, and that the incident beam impinges on the surface of the ac plane.

We use the Miller indices of a face-centered orthorhombic unit cell of the ladder part to denote absolute momentum transfer, $\mathbf{Q} = (H, K, L)$. Because the momentum dependence along the b axis is expected to be very small, we selected the b^* component of the momentum transfer where the scattering angle was close to 90° .

2.3. A pinhole as a post-sample slit system

In Fig. 3(a) the RIXS spectrum measured on a single crystal of the parent compound $\text{Sr}_{14}\text{Cu}_{24}\text{O}_{41}$ at 2 GPa (filled circles) is compared with the spectrum measured away from the sample

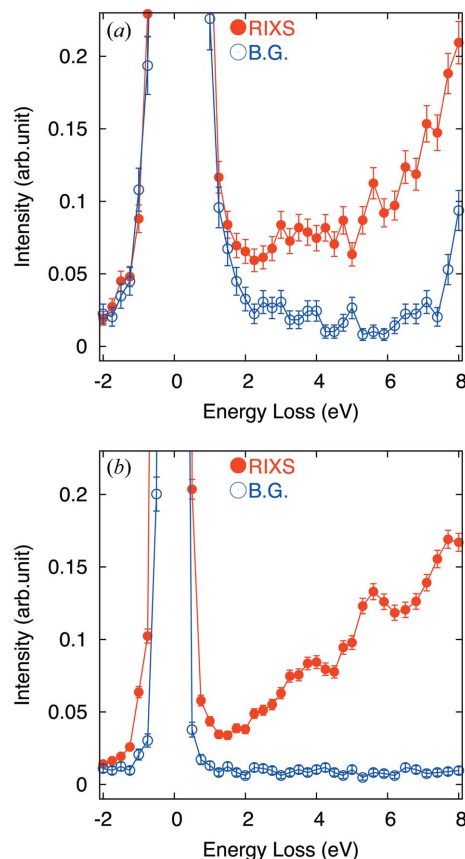


Figure 3
 RIXS spectra under high pressure (a) without and (b) with the post-sample slit. The spectrum with filled circles is RIXS from the sample and the spectrum with open circles is data obtained out of the sample as background.

(open circles), which we use as a background spectrum. The spectrum obtained on the sample in the DAC is clearly different from the RIXS spectra obtained on the same compound at ambient pressure (Ishii *et al.*, 2007), as in the former the elastic peak is asymmetric with a strong tail on the energy-loss side, and the intensity is stronger in the 7–8 eV range. We ascribed these two differences to elastic and inelastic scattering, respectively, from the diamond. Indeed, the incident beam sees the diamond as a point source, and because it is ~ 1 mm away from the sample the resulting elastic scattering deviates to the energy-loss side. Further, the inelastic scattering spectrum of the diamond starts at about 6 eV, which is assigned to an excitation across the band gap of the diamond (Caliebe *et al.*, 2000). In order to reduce the signal from the diamond, we introduced a pinhole (300 μm diameter) as a post-sample slit system (Hiraoka & Cai, 2010), placed as close as possible to the DAC. Its function, schematically represented in Fig. 4, is to act as a collimator that allows the signal of interest to be scattered from the sample and blocks the scattering from the diamond. The effect of the pinhole is illustrated by the RIXS spectra measured on $\text{Sr}_{2.5}\text{Ca}_{11.5}\text{Cu}_{24}\text{O}_{41}$ with the pinhole in Fig. 3(b). The elastic line is symmetric and the intensity around 8 eV disappears in the background spectrum (open) and becomes comparable with the ambient-pressure spectra given by Ishii *et al.* (2007), thus

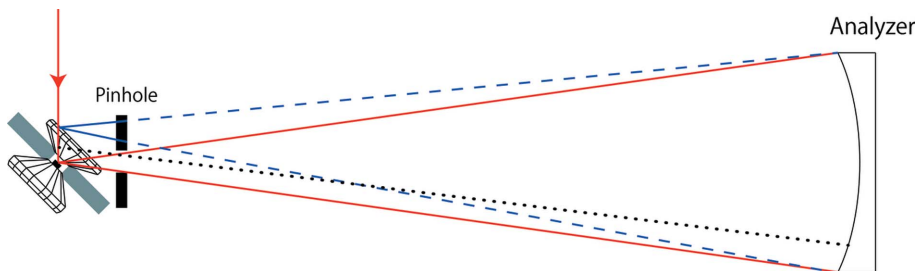


Figure 4
Schematic of the effect of the pinhole placed after the sample. The pinhole acts as a collimator that blocks the scattering from a diamond anvil (dashed lines) and extracts the signal of interest scattered from the sample. Scattered photons produced inside the diamond can still impinge on the analyzer, which is indicated by the dotted line, but it is negligible in the obtained spectra.

highlighting the importance of using the pinhole. One might suspect that this single pinhole cannot shield the scattering from the diamond perfectly. Actually, scattered photons produced inside the diamond can still reach the analyzer, as shown by the dotted line in Fig. 4. In order to shield them completely, one has to assemble two (sample and detector) slits. Alternatively, the scattering from the diamond can be efficiently reduced using the spatial discrimination of a two-dimensional detector, as proposed recently by Verbeni *et al.* (2009). However, as a matter of fact, such scattered photons from inside the diamond are negligible in the spectra in Fig. 3(b). This is because the scattering from the diamond is strongest on its surface. As the incident photons penetrate inside the diamond, the intensity of the scattered photon is reduced. Therefore we conclude that a single pinhole is sufficient to remove the parasitic signal from the diamond for the present study.

3. Results

We measured momentum-resolved RIXS spectra under high pressure by using a single crystal of $\text{Sr}_{2.5}\text{Ca}_{11.5}\text{-Cu}_{24}\text{O}_{41}$. The value of the applied pressure was 3 GPa. Fig. 5(a) depicts the RIXS raw spectra obtained at two momenta, $Q = (0, K, 0)$ and $(0, K, 0.5)$, corresponding to the zone center and zone boundary along the leg direction, respectively. Despite the very low intensity we have succeeded in measuring high-pressure RIXS spectra with reasonable statistics. We also show the raw spectra at ambient pressure at the same momenta in Fig. 5(b). The intensities at the two pressures are substantially different from each other because the spectra at ambient pressure were measured without the DAC. For instance, the intensity of the 3 GPa spectrum becomes about 120 times weaker than that of the ambient-pressure spectrum at the zone center. This

reduction of intensity is due to several factors such as the attenuation of both incident and scattered beams by about 2.828 mm of diamond (~ 0.048), the attenuation of the incident beam by the Be lenses (~ 0.7), the difference in optical path length in air between the ambient- and high-pressure experiments, and also the decrease of the solid angle because of the pinhole.

In order to compare the spectra at 3 GPa and ambient pressure, we normalize the spectral intensity to the integrated intensity at 5–8 eV, based on

the assumption that the spectral weight at high energy loss is unchanged with pressure. In Fig. 5(c) we compare the normalized RIXS spectra at the two momenta. Two excitations in the RIXS spectra of two-leg ladder cuprate were identified in the few-eV region (Ishii *et al.*, 2007). While the intraband excitation in the Zhang–Rice singlet band appears around 1 eV, the excitation across the Mott gap, more precisely an excitation from the Zhang–Rice singlet band to the upper Hubbard band, appears above 2 eV. Differences between the line shapes of the ambient-pressure and the 3 GPa spectra are apparent. For both momenta the two spectra are found to intersect each other at 2 eV. We ascribe this phenomenon to a simultaneous occurrence of an enhancement of the intraband excitation and a change of the excitations across the Mott gap. We note that a similar behavior was observed in the temperature dependence of the RIXS spectra of $\text{Sr}_{14}\text{Cu}_{24}\text{O}_{41}$ (Yoshida *et al.*, 2010). Based on the analogy with the temperature-dependent results, we suggest

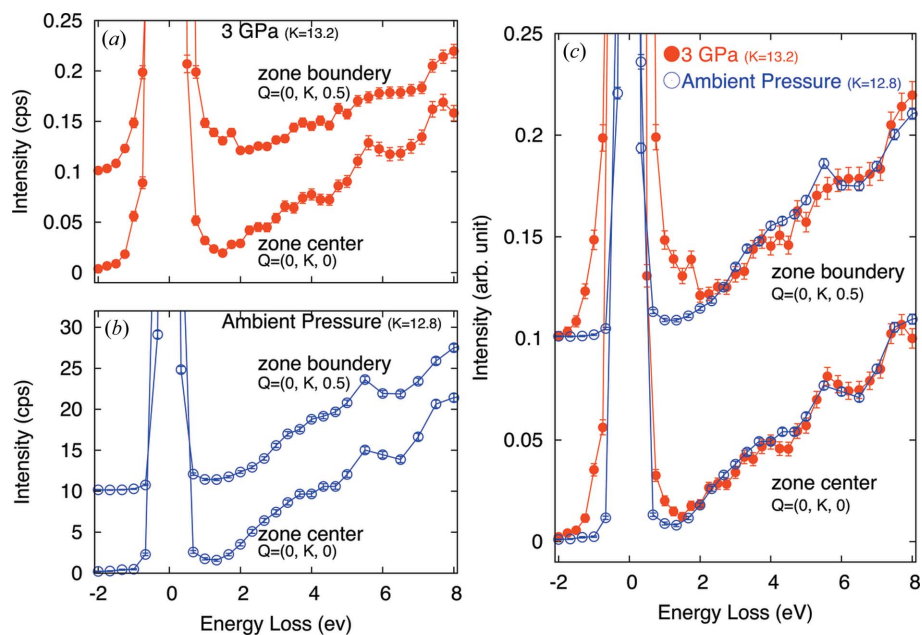


Figure 5
Raw RIXS spectra at the two momenta measured at (a) 3 GPa and (b) ambient pressure. (c) Pressure dependence of RIXS spectra. The spectral intensity is normalized to the integrated intensity at 5–8 eV. For clarity, each spectrum is shifted vertically by 0.1 for (a) and (c), and by 10 for (b) in intensity.

that the high-pressure RIXS data may indicate that the number of holes in the ladders increases with pressure. More work at high pressure is needed to confirm the origin of this behavior.

4. Summary

We have developed the RIXS technique for high-pressure single-crystal experiments. To this end we introduced two devices in a regular optical system at BL11XU, SPring-8: Be lenses and a pinhole. We can obtain better focusing incident X-rays with Be lenses, and, with a pinhole as a post-sample slit system, we could suppress parasitic signals mainly from the diamond. Subsequently, we have performed high-pressure single-crystal RIXS experiments for $\text{Sr}_{2.5}\text{Ca}_{11.5}\text{Cu}_{24}\text{O}_{41}$. We found that changes of the excitations across the Mott gap and enhancement of the intraband excitation occur with pressure qualitatively.

We would like to acknowledge A. Q. R. Baron for the use of the Be lenses and K. Ohwada for technical assistance with the DAC. We thank NSRRC, Taiwan, for providing us with beam time for preliminary experiments at BL12XU/SPring-8. The synchrotron radiation experiments at SPring-8 were performed at BL11XU (proposals Nos. 2010A3502, 2010B3502 and 2011A3502) and BL12XU (proposal No. 2011A4261) with the approval of the Japan Synchrotron Radiation Research Institute (JASRI).

References

- Ament, L. J. P., van Veenendaal, M., Devereaux, T. P., Hill, J. P. & van den Brink, J. (2011). *Rev. Mod. Phys.* **83**, 705.
- Caliebe, W. A., Soininen, J. A., Shirley, E. L., Kao, C.-C. & Hämäläinen, K. (2000). *Phys. Rev. Lett.* **84**, 3907–3910.
- Farber, D. L., Krisch, M., Antonangeli, D., Beraud, A., Badro, J., Occelli, F. & Orlikowski, D. (2006). *Phys. Rev. Lett.* **96**, 115502.
- Hasan, M. Z., Isaacs, E. D., Shen, Z.-X., Miller, L. L., Tsutsui, K., Tohyama, T. & Maekawa, S. (2000). *Science*, **288**, 1811–1814.
- Hemley, R. J., Mao, H.-k., Shen, G., Badro, J., Gillet, P., Hanfland, M. & Häusermann, D. (1997). *Science*, **276**, 1242–1245.
- Hill, J. P., Blumberg, G., Kim, Y.-J., Ellis, D. S., Wakimoto, S., Birgeneau, R. J., Komiya, S., Ando, Y., Liang, B., Greene, R. L., Casa, D. & Gog, T. (2008). *Phys. Rev. Lett.* **100**, 097001.
- Hiraoka, N. & Cai, Y. Q. (2010). *Synchrotron Radiat. News*, **23**, 26–31.
- Ishii, K., Ishihara, S., Murakami, Y., Ikeuchi, K., Kuzushita, K., Inami, T., Ohwada, K., Yoshida, M., Jarrige, I., Tatami, N., Niioka, S., Bizen, D., Ando, Y., Mizuki, J., Maekawa, S. & Endoh, Y. (2011). *Phys. Rev. B*, **83**, 241101.
- Ishii, K., Tsutsui, K., Tohyama, T., Inami, T., Mizuki, J., Murakami, Y., Endoh, Y., Maekawa, S., Kudo, K., Koike, Y. & Kumagai, K. (2007). *Phys. Rev. B*, **76**, 045124.
- Kao, C.-C., Caliebe, W. A. L., Hastings, J. B. & Gillet, J.-M. (1996). *Phys. Rev. B*, **54**, 16361.
- Kim, Y.-J., Hill, J. P., Yamaguchi, H., Gog, T. & Casa, D. (2010). *Phys. Rev. B*, **81**, 195202.
- Kojima, K. M., Motoyama, N., Eisaki, H. & Uchida, S. (2001). *J. Electron Spectrosc. Relat. Phenom.* **117–118**, 237–250.
- Loa, I., Lundegaard, L. F., McMahan, M. I., Evans, S. R., Bossak, A. & Krisch, M. (2007). *Phys. Rev. Lett.* **99**, 035501.
- Piermarini, G., Block, S., Barnett, J. & Forman, R. (1975). *J. Appl. Phys.* **46**, 2774–2780.
- Protopopov, V. & Valiev, K. (1998). *Opt. Commun.* **151**, 297–312.
- Raymond, S., Bouchet, J., Lander, G. H., Le Tacon, M., Garbarino, G., Hoesch, M., Rueff, J.-P., Krisch, M., Lashley, J. C., Schulze, R. K. & Albers, R. C. (2011). *Phys. Rev. Lett.* **107**, 136401.
- Raymond, S., Rueff, J.-P., D'Astuto, M., Braithwaite, D., Krisch, M. & Flouquet, J. (2002). *Phys. Rev. B*, **66**, 220301.
- Rueff, J.-P. & Shukla, A. (2010). *Rev. Mod. Phys.* **82**, 847–896.
- Sasaki, S. (1990). *KEK Report* 90–16, pp. 1–143. KEK, Japan.
- Shukla, A., Rueff, J.-P., Badro, J., Vanko, G., Mattila, A., de Groot, F. M. F. & Sette, F. (2003). *Phys. Rev. B*, **67**, 081101.
- Snigirev, A., Kohn, V., Snigireva, I. & Lengeler, B. (1996). *Nature (London)*, **384**, 49–51.
- Verbeni, R., Pylkkänen, T., Huotari, S., Simonelli, L., Vankó, G., Martel, K., Henriquet, C. & Monaco, G. (2009). *J. Synchrotron Rad.* **16**, 469–476.
- Yoshida, M., Ishii, K., Ikeuchi, K., Jarrige, I., Murakami, Y., Mizuki, J., Tsutsui, K., Tohyama, T., Maekawa, S., Kudo, K., Koike, Y. & Endoh, Y. (2010). *Physica C*, **470**, S145–S146.